Journal of Applied Polymer Science

Structure and properties of a low viscosity acrylate based flexible epoxy resin

Yuan Yang,[1] Yun-Feng Zhao,[2] Jian-Yue Wang,[2] Chuan Zhao,[2] Liu Tong,[2] Xiao-Yan Liu,[2] Ji-Hua Zhang,[2] Mao-Sheng Zhan[1]

[1]Key Laboratory of Aerospace Materials and Performance (Ministry of Education), School of Materials Science and Engineering, Beihang University, Beijing, China

[2]Aerospace Research Institute of Materials and Processing Technology, Beijing 100076, China

Correspondence to: Y. Yang (E-mail: yangyuan3001@163.com)

ABSTRACT: A series of low viscosity acrylate-based epoxy resin (AE)/glycol diglycidyl ether (GDE) systems were prepared. The effect of GDE and low molecular weight polyamide (LPA) content on the rheological behavior, phase structure, damping, and mechanical properties were studied by differential scanning calorimeter (DSC), viscometer, scanning electron microscopy (SEM), dynamic mechanical thermal analysis (DMTA), and electro mechanical machine. The viscosity of the uncured AE systems decreased significantly after the incorporation of GDE. The damping properties were found to decrease slightly with the increasing GDE and LPA content. The tensile strength of the cured AE/GDE samples enhanced significantly after the incorporation of GDE with at least 150% improvement for all the samples while it decreased slightly with increasing LPA content. The AE/GDE cured systems were intended for future use as structural damping materials. © 2015 Wiley Periodicals, Inc. J. Appl. Polym. Sci. **2016**, *133*, 42959.

KEYWORDS: elastomers; mechanical properties; resins; thermosets; viscosity and viscoelasticity

Received 27 July 2015; accepted 21 September 2015

DOI: 10.1002/app.42959

INTRODUCTION

Damping systems play an important role in the field of high performance structural application on aerospace, marine, automobile and construction, etc.[1,2] Epoxy resins are usually applied as protective coating, adhesives, electronic-packaging materials, and composites matrix for their excellent chemical resistance, adhesion, dimensional stability, and mechanical properties.[3,4] However, the drawbacks, such as poor damping properties and brittleness, which was caused by the high crosslink density, restricted their applications. For recent years, great efforts have been done to modify the damping properties of epoxy resins.[5–8] The most common method to enhance the damping of epoxy resin was to add a second phase, such as rubbers,[5,9,10] thermoplastic polymers,[6,11,12] and inorganic fillers,[7,13–15] which can form a multiphase morphology or semi-interpenetrating polymer network.[8,16–18] The excess energy loss, attributing to phase separation, plastic deformation, and interface fraction between fillers and fillers or matrix, will improve the damping property of epoxy resin system. Rheological behavior of uncured resin is one important parameter for the processing of thermosetting matrix in applications such as composite matrix. While, it will lead to the increase in viscosity[19,20] to incorporate rubbers, thermoplastic polymers, or inorganic fillers into epoxy resin matrix. The improved viscosity may limit the application of the modified damping matrices.

Beside above mentioned, modification on resin structure, such as incorporating flexible backbone structure, which can decrease the crosslink density of a cured epoxy resin system, will be also an effective method to improve its damping properties, which would not lead to significant phase separation and increase in viscosity. Grant *et al.*[21] used a viscoelastic RF-69 as chain extension modifier (RF-69) to prepare intrinsic epoxy resin damped composites, and the results showed that the damped composite improved significantly. Wang *et al.*[22,23] used amino-terminated polyether and amino-terminated polyurethane as curing agent to prepare flexible epoxy resin damping systems, and the results showed that the highest loss factor had reached 1.57, indicating the epoxy resin system with pretty damping properties. Ratna *et al.*[24] used polyether amine hardeners with varying chain lengths of polyether as cure agent to prepare flexible epoxy resin damping systems, and the results showed that the highest loss factor was around 1.9, with tensile strength from 14.8 to 0.5 MPa and elongation at break from 50 to 210% when the chain length increases. However, little researches about the rheological behavior of damping epoxy resin matrices have been reported yet.

© 2015 Wiley Periodicals, Inc.

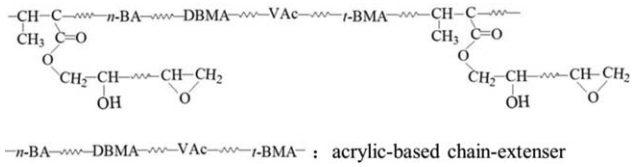

Figure 1. Structure of acrylic-based epoxy resin.

In this study, a low viscosity acrylate-based epoxy resin/GDE system was prepared. The primary aim of this work was to evaluate the effect of GDE and LPA content on the viscosity, cure behavior, morphology, damping properties, and mechanical properties of epoxy resin and its potentiality as a damping composite matrix. The rheologic properties and cure behavior were evaluated through viscosity and dynamic DSC measurements. The damping and mechanical properties were studied to estimate the effect of various GDE content, cure agent content, and post cure temperature on the above properties. Microscopy was used to investigate fracture surfaces of all cured sample prepared under various conditions.

EXPERIMENT

Materials

Acrylic-based epoxy resin (AE) was prepared in ourselves laboratory, whose structure was shown in Figure 1. Glycol diglycidyl ether (GDE) was supplied by Changshu Hengrong commerce and trade. Low molecular weight polyamide resin (LPA) supplied by Shanghai Resin (China) was used as curing agent in a weight ratio of 100/50, i.e. 50 phr (parts per hundred epoxy resin). All of the agents were used as received without further purification.

Table I. Recipe of AE/GDE/LPA Samples

Sample no.	AE (g)	GDE (g)	LPA (g)	Cure process (g)
GDE-0	100	0	50	Cure 2
GDE-10	100	10	50	Cure 2
GDE-20 (LPA-50, cure-2)	100	20	50	Cure 2
GDE-30	100	30	50	Cure 2
GDE-40	100	40	50	Cure 2
GDE-50	100	50	50	Cure 2
LPA-40	100	20	40	Cure 2
LPA-60	100	20	60	Cure 2
LPA-70	100	20	70	Cure 2
cure-1	100	20	50	Cure 1
cure-3	100	20	50	Cure 3

Cure 1: 70°C/1 h+100°C/3 h; Cure 2: 70°C/1h+100°C/1h+130°C/2h; cure 3: 70°C/1 h+100°C/1 h+130°C/1 h+180°C/1 h.

Preparation of Samples

AE (100 g) and GDE (20 g) were charged in a beaker, and stirred for 15 min at room temperature. Then LPA (250 g) was

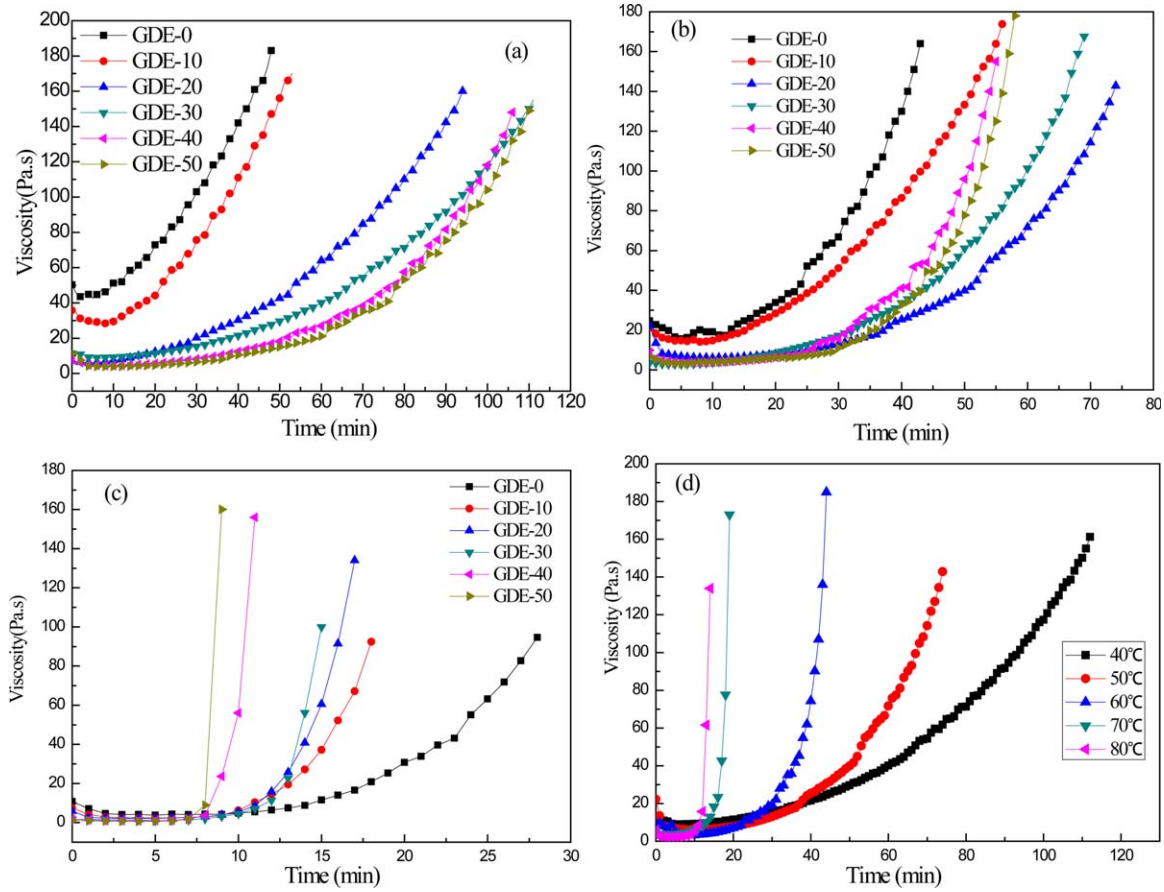

Figure 2. Effect of GDE content on the rheological behavior of AE-40/LPA systems (a) 40°C; (b) 50°C; (c) 80°C; (d) 20 phr GDE content. [Color figure can be viewed in the online issue, which is available at wileyonlinelibrary.com.]

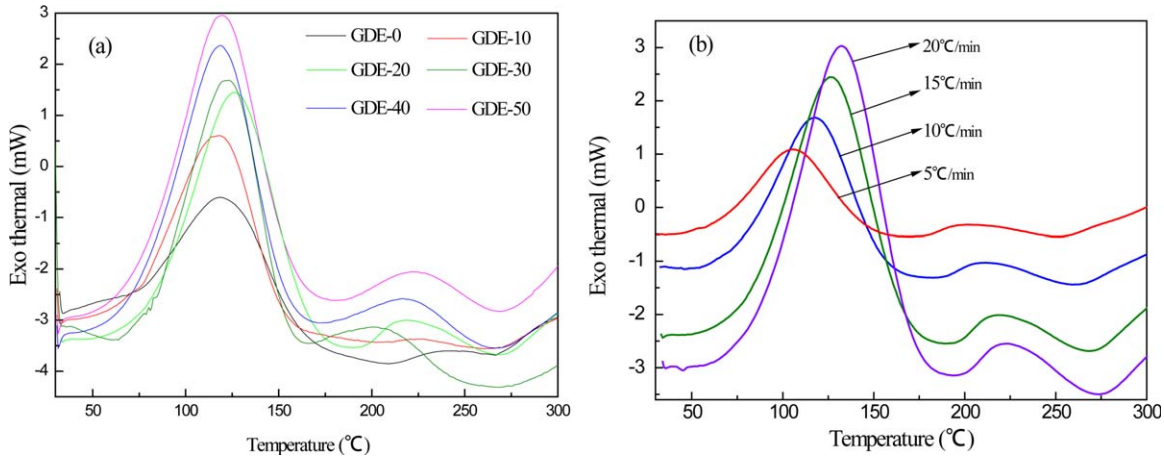

Figure 3. DSC curves of AE-40/PLA systems with (a) various GDE content at 15°C min^{-1}; (b) 20 phr. DEG at various heating rate. [Color figure can be viewed in the online issue, which is available at wileyonlinelibrary.com.]

added and stirred for another 15 min at room temperature. The epoxy/LPA blends was degassed in vacuum drying chamber for 30 min and then poured into a preheated mold, followed by being cured at 70°C for 1 h, 100°C for 1 h, and 130°C for 2 h, then cooling down to room temperature. The rest samples were prepared following recipes in Table I.

Characterization

Rheological Behavior. The rheologic tests were performed on a Brookfield Programmalbe DV-II Viscometer. The isothermal viscosity was taken during 40–80°C with 10°C one stage.

Differential Scanning Calorimeter. A differential scanning calorimeter (Metteler Toledo DSC 1 Stare System) was used for dynamic DSC measurements under N_2 atmosphere. Dynamic DSC measurements were carried out at 5, 10, 15, 20°C min^{-1} for the AE-20, AE-30, and AE-40/PLA uncured systems.

Dynamic Mechanical Thermal Analysis (DMTA). Dynamic mechanical thermal analysis (DMTA) was carried out using a DMTA VA4000 (Metravib R.D.S.) by using a tensile clamp and the testing method of temperature step-frequency sweep with a temperature step of 2°C and a frequency range between 10 and 100 Hz. The testing was carried out according to ISO 4664-1-2005. The sample dimensions were 20-mm long, 6-mm wide, and 2-mm thick. The storage modulus E', the loss modulus E'', and the loss factor (tan δ) could be obtained from the testing, and the peak temperature of tan δ is taken as the glass transition temperature.

Mechanical Testing. The tensile tests were carried out on an electro-mechanical machine (Sintech65/G, MTS), using dumbbell shaped type sample according to ISO 7619-1-2004. Five samples were tested per material. The hardness was performed on a Shore A durometer according to ISO 48-2010. All samples were evaluated without any condition.

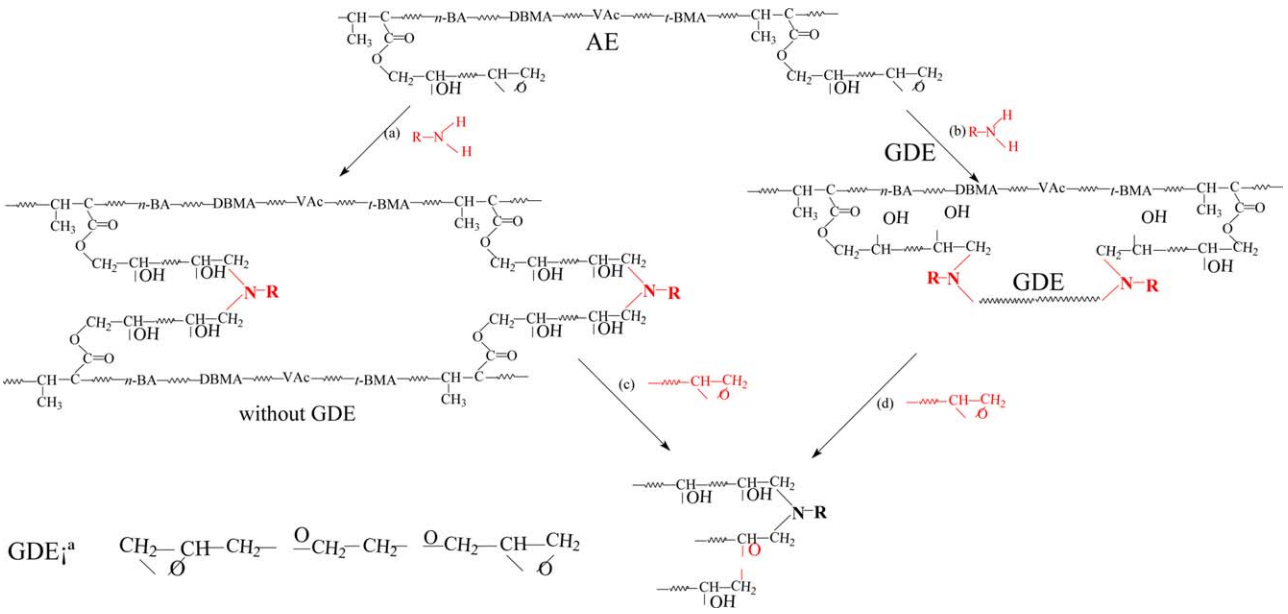

Figure 4. Reaction mechanisms of AE/GDE blends. [Color figure can be viewed in the online issue, which is available at wileyonlinelibrary.com.]

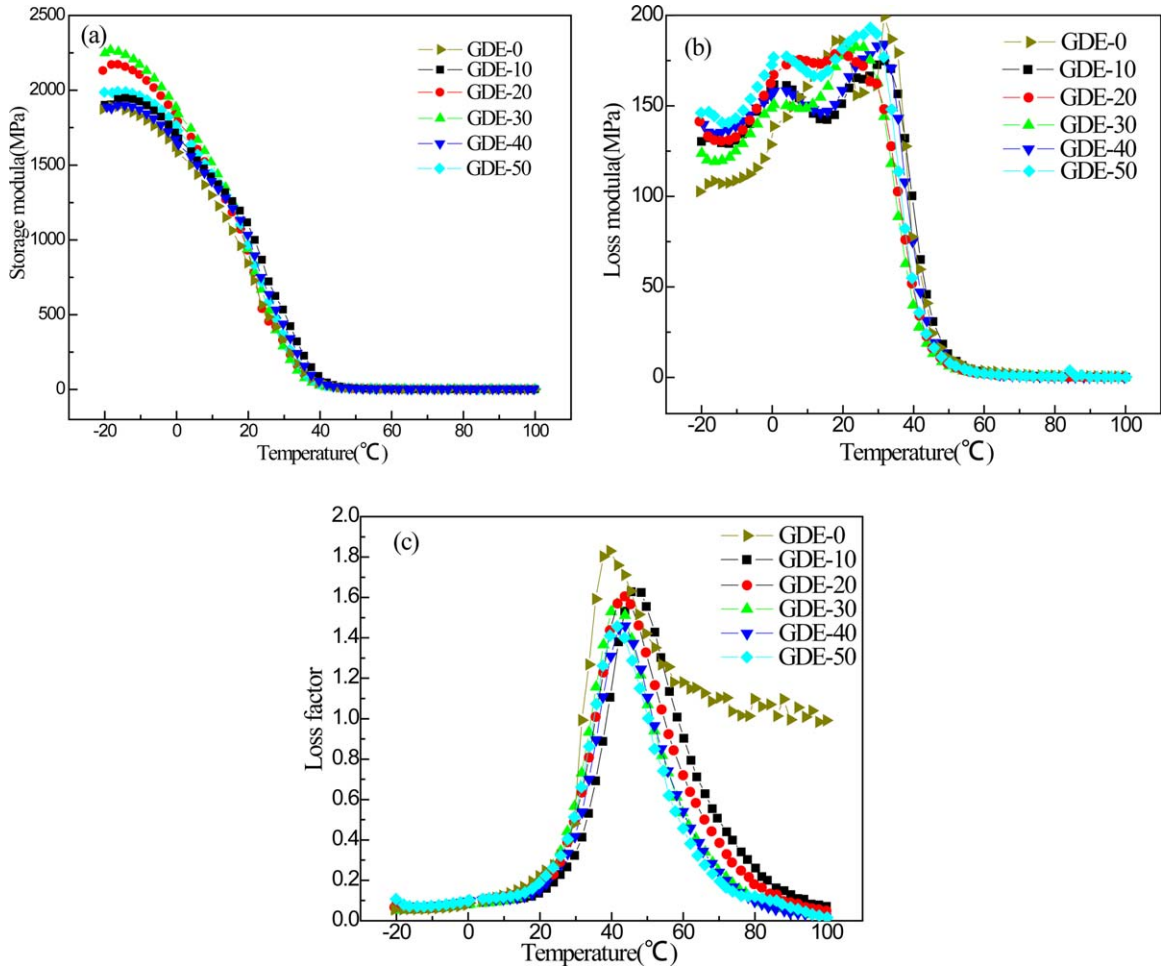

Figure 5. DMTA plots of AE with various GDE content at 10 Hz. [Color figure can be viewed in the online issue, which is available at wileyonlinelibrary.com.]

Scanning Electron Microscopy. Morphology of cured AE samples was performed on a scanning electron microscope with an acceleration voltage of 20 KV. The samples were fractured in liquid nitrogen. Before examination, all the fracture surfaces were sputtered-coated with gold.

RESULTS AND DISCUSSION

Rheological Behavior

Isothermal viscosity measurements were performed on a viscometer, and the corresponding results were shown in Figure 2(a–d), respectively. The isothermal viscosity curves of AE/LPA system with various GDE content at 40, 50, and 80°C were illustrated in Figure 2(a–c), and it was clear that the viscosity of AE/LPA systems with the increasing GDE content from 0 to 50 phr, showed a significant decrease attributing to the flowability of GDE. The initial viscosity decreased significantly while the cure rate was accelerated with GDE content increasing from 0 to 50 phr, especially at higher temperature. Incorporation of GED or improving temperature will expand the "free volume" of the AE molecular and weaken the reaction between macromolecular chains, which may result in the decrease of viscosity. At the same time, an interesting phenomenon was that the isothermal viscosity rising rate showed an inverse trend at higher temperature [Figure 2(c)] and lower temperature [Figure 2(a)]. For this result, it might be attributed to the two aspects of temperature and crosslink density.[25,26] With increasing temperature, the viscosity decreases, on the contrary, the reaction rate is accelerated, which will lead to viscosity increase, due to increase in crosslink density caused by reaction. At lower temperature, the temperature is the main factor; while the crosslink density takes the major place on the viscosity increase. This can explain why the inverse trends happened at various testing temperature. The viscosity curves of AE/LPA system with 20 phr GDE at various temperatures were shown in Figure 2(d), which confirm the results above discussed.

Curing Behavior

The curing behavior of AE/PLA blends with various GDE content was conducted with various heating rates of 5, 10, 15, and 20°C min^{-1}. The dynamic DSC curves of AE/PLA blends with various GDE content were shown in Figure 3(a), and the DSC curves of AE/PLA blends with 20 phr GDE under various heating rates were shown in Figure 3(b), and the cure mechanism was shown in Figure 4. From Figure 3(a,b), it was clear that two exothermic peaks were noted in the DSC curves, the stronger one appearing at lower temperature and the other one at higher

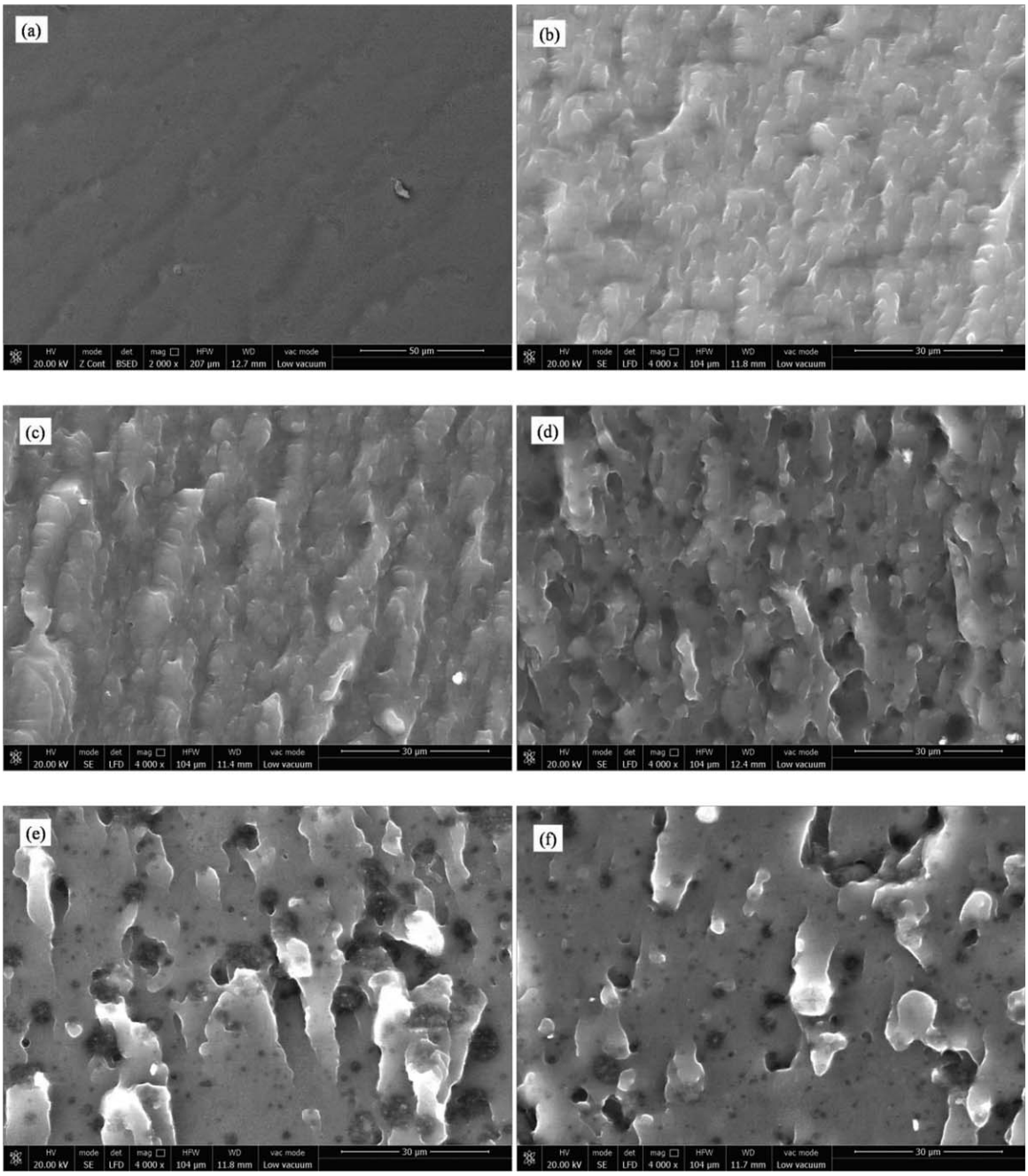

Figure 6. Frozen fracture morphology from AE cured samples with (a) 0 phr GDE content; (b) 10 phr GDE content; (c) 20 phr GDE content; (d) 30 phr GDE content; (e) 40 phr GDE content; (f) 50 phr GDE content.

position. It was also found that both the exothermal peaks shifted toward higher temperature side with the increasing heating rate.

It is well known that exothermic peaks are associated with the curing reaction in the epoxy resin system.[27] As it can be seen from the Figure 3, the stronger exothermic peaks at lower temperature were corresponding to the main curing reaction between epoxy groups and cure agent, and the weaker one at higher temperature might be associated with the reaction between epoxy groups and hydroxy groups, which was consonance with the reference.[28]

Dynamic Mechanical Thermal Analysis

The dynamic mechanical properties of AE were determined by dynamic mechanical thermal analysis. The plots of E', E'', and tan δ for AE cured samples, prepared under various conditions, were listed in Figures 5–8, and the corresponding data collected in Table II.

Effect of GDE Content on the Dynamic Mechanical Properties. Figure 5 showed the temperature dependence of E', E'', and tan δ for cured AE with various GDE content. As shown in Figure 5(a), the E' increased from 1800 to 2270 MPa when GDE content increased from 10 to 30 phr, and then

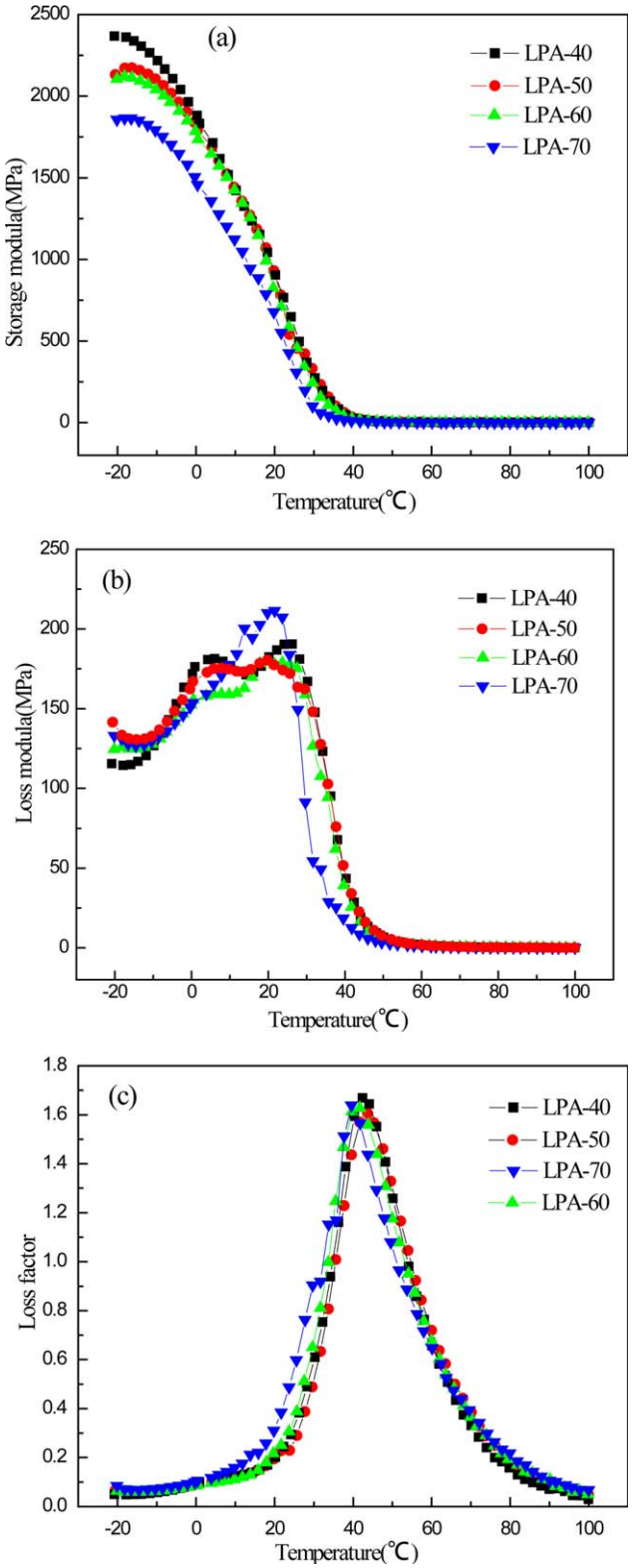

Figure 7. DMTA plots of AE with various LPA content at 10 Hz. [Color figure can be viewed in the online issue, which is available at wileyonlinelibrary.com.]

decreased to 1900 MPa. As shown in Figure 5(c), the value of tan δ exhibited a decrease during the rubber region with the increasing GDE content from 0 to 50 phr, while both the T_g value and storage modulus in glassy region showed a trend of first increase followed by decrease with the GDE content increase. The T_g increased from 39 to 47°C when GDE 10 phr content was incorporated, and then gradually decreased to 42°C when GDE content further increased to 50 phr. The main reason for this phenomenon may be attributed to the following reasons. First, GDE, with short flexible molecular chain segments, participated in the crosslink of AE/LPA systems, which will significantly improve the crosslink density. Second, the increasing GDE content may also improve the crosslink density, which could increase the E' of AE/LPA samples, too. Third, the short molecular chain segment of GDE, filled in the voids of the large AE molecular, can also improve the E' during glassy region. On the contrary, at higher temperature, the small molecular will improve the motion ability of polymer chains segments, which explain the decrease in E' and T_g with increasing GDE content.

The fracture morphology micrographs of AE cured samples with various GDE content were illustrated in Figure 6. The frozen fracture surface micrograph of sample without GDE was illustrated in Figure 6(a), showing a clear homogeneous phase. With the increasing GDE content from 10 to 50 phr, the fracture surface micrographs were shown in Figure 6(b–f), which exhibited typical toughed fracture with significant shear yielding. As shown in Figure 6(b–f), cellular phase structures were observed with significant shear yielding and corresponding holes without significant phase separation. The curves of loss factor dependant on temperature, with only one peak, implied a homogenous phase structure for the samples, which confirmed the results of fracture surface micrographs. The cured AE system was comprised of soft chain segments and hard chain segments, which might result in the splitting of loss modulus curves. This might be attributed to the quasi co-continuous phase structure comprised of matrix and GDE rich phase, just as described in earlier reference.[29,30]

Effect of LPA Content on the Dynamic Mechanical Properties. Figure 7 shows the temperature dependence of E', E'', and tan δ for cured GDE-20 content with various LPA content. From the Figure 7(a), it was clear that the E' of the cured GDE-20, with the increasing LPA content, decreased gradually during glassy region. While the "valley" in the curves of E'' disappeared with the increasing LPA content as shown in Figure 7(b). The tan δ results from Figure 7(b) indicated that the T_g shifted to lower temperature with the increasing LPA content. The main reason for these results can be attributed to the following aspects. With increasing LPA content from 40 to 70 phr, the LPA may be excessive, which can decrease the crosslink density and lead to the improvement of molecular chain motion ability. The above results could be confirmed by the fracture morphology micrographs shown in Figure 8.

The fracture morphology micrographs of AE cured samples with various LPA content were illustrated in Figure 8. From the micrographs in Figure 8, massive shear yielding was observed, revealing a typical toughness character, while the fracture became smooth gradually, with the increasing LPA content, attributing to the compatibility modification of LPA. The result

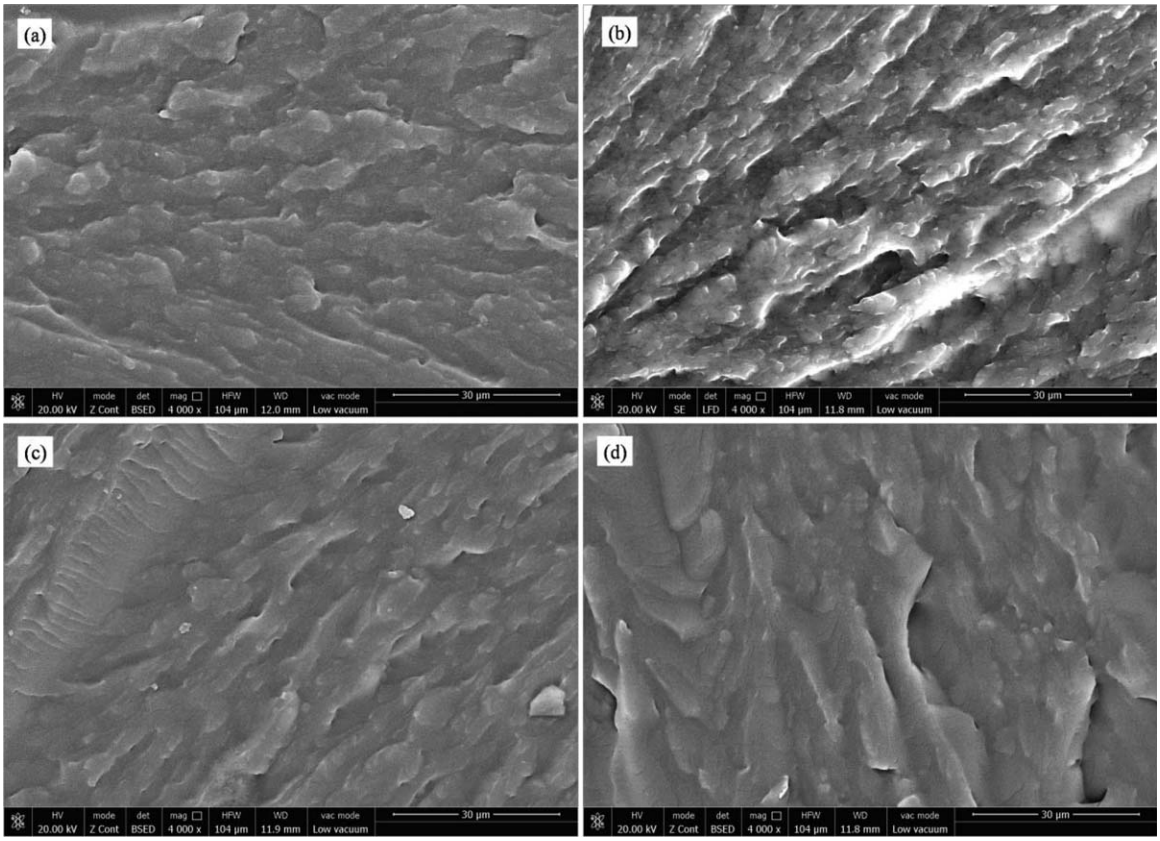

Figure 8. Frozen fracture morphology from AE cured samples with (a) 40 phr LPA content; (b) 50 phr LPA content; (c) 60 phr LPA content; (d) 70 phr LPA content.

was corresponding to the plots of E'' vs. temperature, that the hollowness was flatted with the increasing LPA content.[31]

Effect of Post Cure Temperature on the Dynamic Mechanical Properties. Figure 9 showed the temperature dependence of E', E'', and tan δ for cured AE with various post cure temperature. From Figure 9(a), it was clear that the E' enhanced significantly when samples cured at higher temperature. The plots of E'' dependant on temperature were illustrated in Figure 9(b). From Figure 9(b), it revealed that a secondary peak emerged gradually and the viscoelastic region shifted to higher temperature with increasing post cure temperature. As shown in Figure 9(c), the T_g of the cured AE systems shifted to higher temperature, while the value of tan δ decreased gradually with the increasing post cure temperature. The tan δ values of the cured samples were 1.75, 1.61, and 1.46, when the post cure temperature increased from 130 to 180°C. The T_g values of the cured AE systems, with increasing post curing temperature, were determined to be 39.8, 43.9, and 49.5°C, respectively. An increase about 10°C in the glass transition temperature was achieved with the higher post cure procedure.

This could be explained by the contribution of crosslink density of the cured AE systems. It was noteworthy that undergoing post curing treatment at higher temperature mainly had an effect on the crosslinking density of the cured AE systems through the contribution of the etherification reaction at elevated temperature, which was consonance with the reference.[32,33]

The fracture morphology micrographs of AE cured samples at various post cure temperature were illustrated in Figure 10. As shown in Figure 10, massive of shear yielding, comprised of "ridges" and "valleys," was observed, exhibiting a quasi co-continuous phase structure, corresponding to the two E'' peaks while single loss factor peak. At higher post cure temperature,

Table II. Dynamic Mechanical Properties Cured AE-40 Systems

Samples	tan δ_{max}	T_g (°C)	Temp. range of tan $\delta > 0.3$ (°C)	$\triangle T_{\tan\delta > 0.3}$ (°C)
GDE-0	1.84	39.7	26.0–100	>74.0
GDE-10	1.63	45.7	29.0–78.3	49.3
GDE-20 (LPA-50, cure-2)	1.61	43.9	25.9–73.2	47.3
GDE-30	1.56	41.8	23.4–68.6	45.2
GDE-40	1.46	43.6	27.3–67.0	49.7
GDE-50	1.46	41.2	25.2–64.6	39.4
LPA-40	1.67	42.4	24.3–71.5	47.2
LPA-60	1.63	41.8	23.4–74.1	50.7
LPA-70	1.64	39.7	19.6–73.6	54.0
Cure-1	1.74	40.1	22.6–71.6	49.0
Cure-3	1.45	49.5	28.8–79.4	50.6

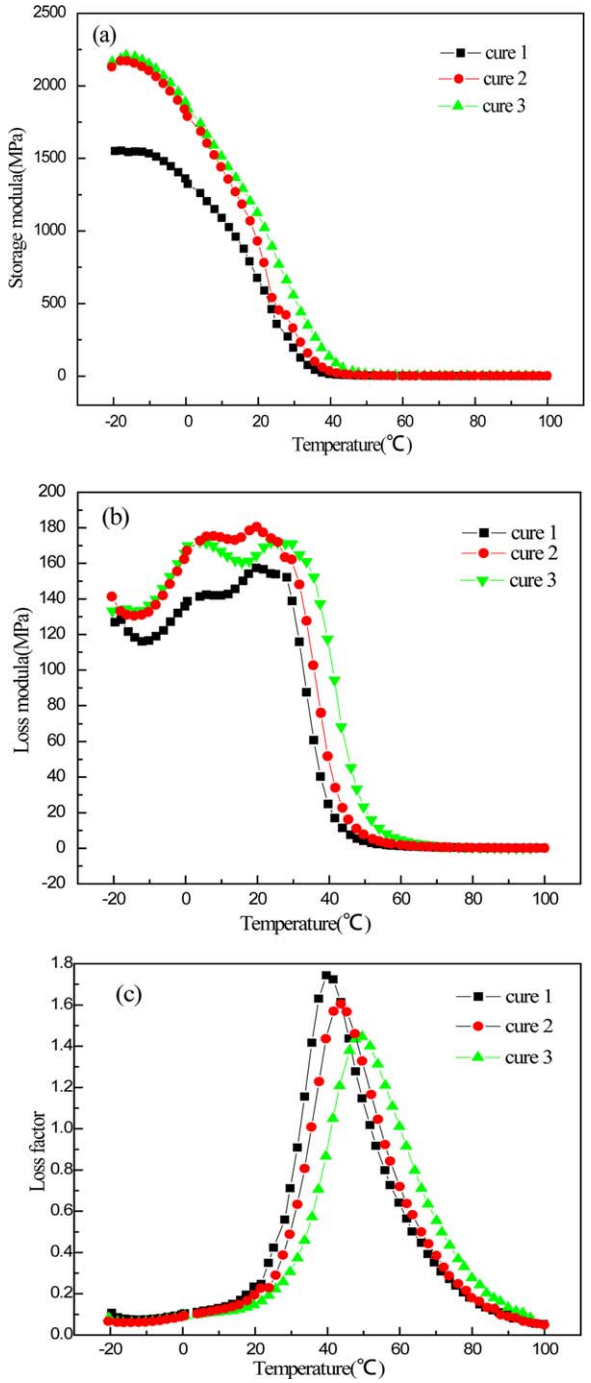

Figure 9. DMTA plots of cured AE with various post cure temperature at 10 Hz. [Color figure can be viewed in the online issue, which is available at wileyonlinelibrary.com.]

the shear yielding became more concentrated than those prepared at lower temperature, which was attributed to the decrease in motion of chain segments caused by the crosslink density improvement.

Effect of Testing Frequency on the Dynamic Mechanical Properties. The temperature dependence of tan δ for cured AE/LPA with 20 phr GDE (GDE-20) at different frequencies was given in Figure 11. It can be seen in the curves, there was a single glass transition peak for the samples at around 36°C, which shifted to higher temperature with the increasing testing frequency. This phenomenon can be explained by time-temperature superposition (TTS) principle,[34,35] which confirmed the results reported in references.[8,18]

Mechanical Properties

The mechanical properties of cured AE systems, including tensile strength, elongation at break and hardness, were determined by tensile tester and Shore durometer. The effects of GDE content, LPA content, and post cure temperature were investigated. The results were collected in Table III. The mechanical properties of AE cured system depended on the rigidity of molecular

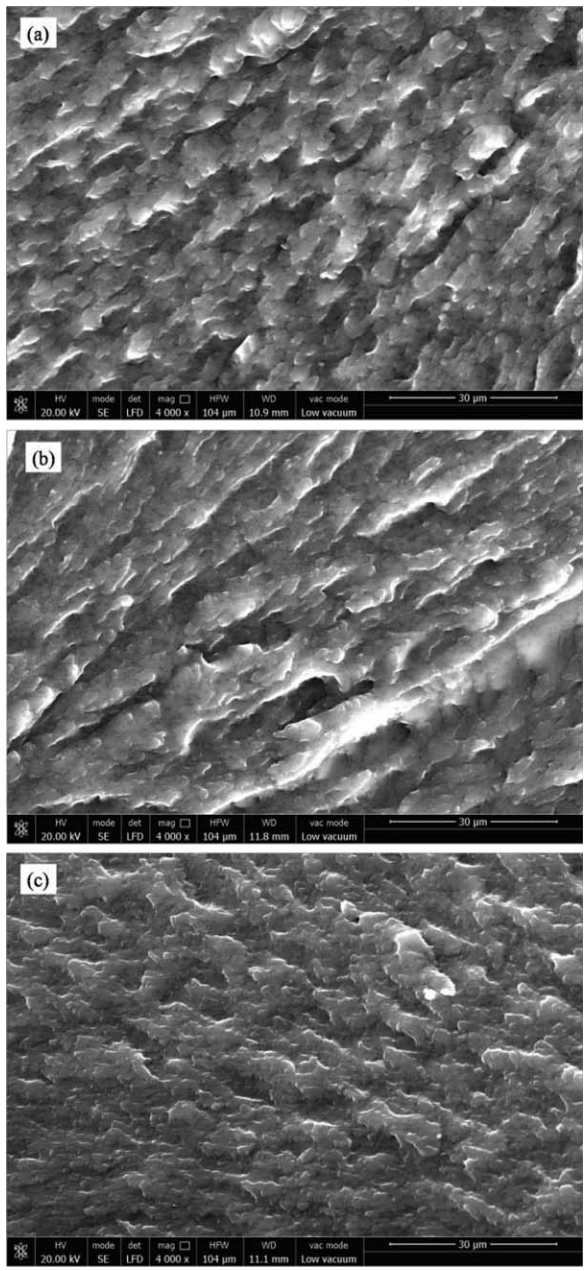

Figure 10. Frozen fracture morphology from AE cured samples at (a) cure 1; (b) cure 2; (c) cure 3.

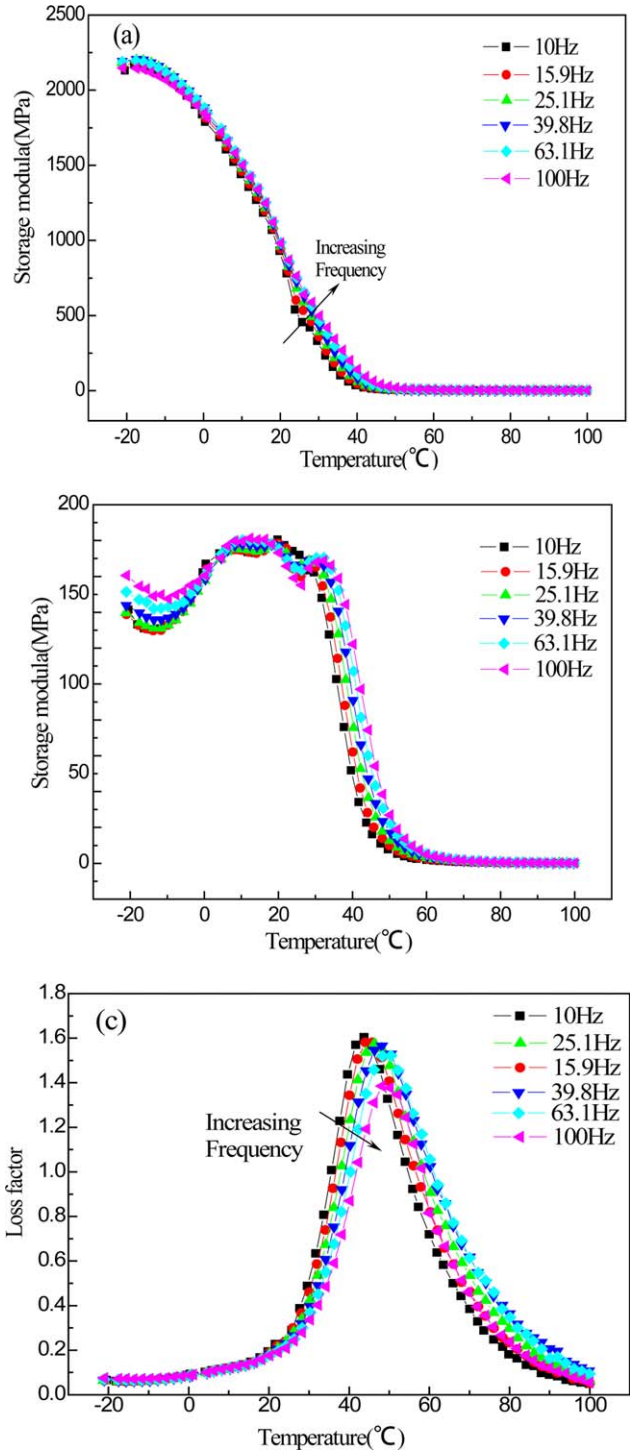

Figure 11. DMTA plots of cured AE at different frequencies with 20 phr GDE content. [Color figure can be viewed in the online issue, which is available at wileyonlinelibrary.com.]

chains and the crosslink density. Generally, flexible additives will decrease the mechanical properties of cured AE samples; however, improve the motion of polymer chain segment.

Effect of GDE Content on the Mechanical Properties. The mechanical properties of cured AE/LPA samples with various GDE content were illustrated in Figure 12(a,b) and the corresponding data was collected in Table III. As above mentioned, flexible additives will decrease the mechanical properties, however, improve the motion of polymer chain segment. It was interesting to find that the tensile strength of cured AE systems improved at least 150% when GDE of various contents was added. When GDE content was only 10 phr, the tensile strength improved from 6.50 to 23.4 MPa, with a dramatic 265% improvement. When the GDE content increased from 10 to 50 phr, the tensile strength showed a trend of first decrease and then followed by an increase, while the elongation at break and hardness exhibited an opposite trend with the increasing GDE content from 10 to 50 phr. The main reason for the above phenomenon might be attributed to the following aspects. First, as above mentioned, the flexible short chain segment of GDE can significantly improve the crosslink density, which can restrict the motion of molecular chain, leading to the surprising improvement in tensile strength and decrease in elongation at break. Second, when the GDE content was low (from 10 to 30 phr), GDE was mainly utilized as flexible additives, which led to the decrease in tensile strength and enhancement in elongation at break. With the increasing GDE content from 30 to 50 phr, the GDE played a more important role in improving the crosslink density, which led to the increase in tensile strength and decrease in elongation at break.

Effect of LPA Content on the Mechanical Properties. The mechanical properties of AE samples with 20 phr GDE content and various LPA content were illustrated in Figure 12(c,d) and Table III. As shown in Figure 12(c,d), the tensile strength decreased from 21.5 to 12.0 MPa. On the contrary, the elongation at break enhanced from 40.4 to 164%. While, the hardness exhibited a trend of first improve from 95 to 97 and then followed by a decrease (to 92) when LPA content was over 60 phr. The results could be attributed to the following aspects. LPA, with plenty flexible chain segments, plays an important role in improving the flexibility of AE cured systems. Increasing LPA content might decrease the crosslink density. Moreover,

Table III. Mechanical Properties Cured AE-40 Systems

Samples	Hardness	Tensile strength (MPa)	Elongation at break (%)
GDE-0	93	6.50	185
GDE-10	97	23.4	6.00
GDE-20 (LPA-50, cure-2)	97	19.6	71.2
GDE-30	97	16.3	88.1
GDE-40	96	20.3	39.3
GDE-50	95	26.0	16.6
LPA-40	95	21.5	40.4
LPA-60	97	17.2	117
LPA-70	92	12.0	164
Cure-1	97	14.2	105
Cure-3	97	30.3	12.5

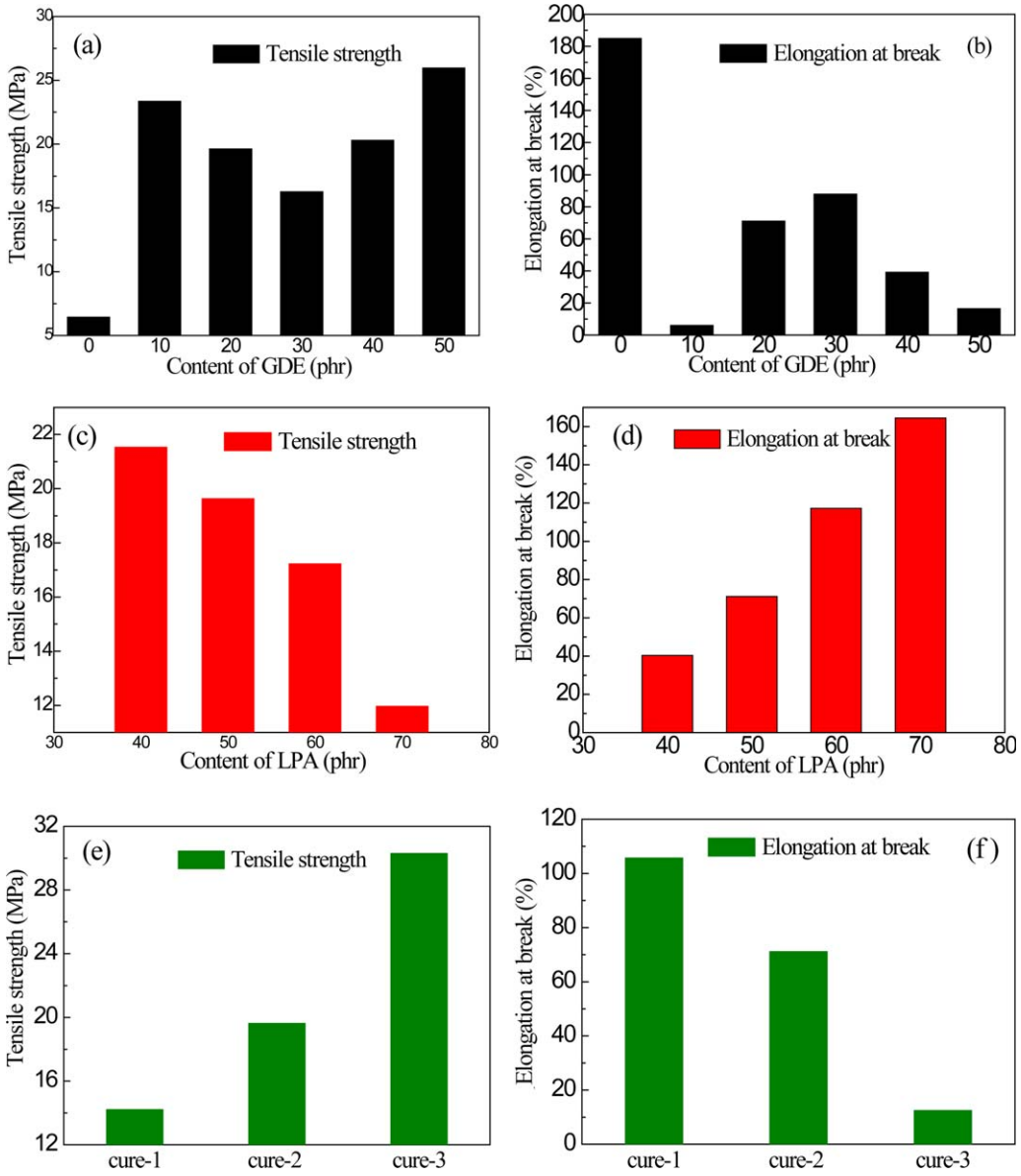

Figure 12. Mechanical properties of cured AE with various: (a) and (b) GDE content; (c) and (d) LPA content; (e) and (f) post cure temperature. [Color figure can be viewed in the online issue, which is available at wileyonlinelibrary.com.]

increasing LPA content might introduce too much flexible units, which might lead to enhancement on motion of molecular chain segments. Both of the incorporation of flexbile chain segments and decrease in crosslink density would decrease the tensile strength and improve the elongation at break.

Effect of Post Cure Temperature on the Mechanical Properties. The mechanical properties of AE sample under various post cure temperature were illustrated in Figure 12(e,f) and Table III. As shown in Figure 12(e,f), the tensile strength enhanced from 14.22 to 30.33 MPa, on the contrary, the elongation at break decreased from 105.9 to 12.5%, which can be attributed to the improved crosslink density with increasing post cure temperature. The improved crosslink density will restrict the molecular chain motion, leading to the above phenomenon.

CONCLUSIONS

In this article, effect of GDE and LPA content on the phase structure, rheological behavior, damping, and mechanical properties were investigated. Incorporation of GDE at various contents (0–50 phr) into AE matrix significantly decreased the viscosity of AE/GDE systems, which made the damping matrix more flowable and processable. The DMTA results showed that the cured AE samples exhibited excellent damping properties, with a highest loss factor value of 1.75, and the corresponding temperature range of tan δ>0.3 was over 50°C, while, the loss factor value showed a slight decrease with increasing LPA content. At the same time, the tensile strength of the cured samples could reach

30.3 MPa, with at least 150% improvement for all the samples, as comparing with the samples without GDE, however, the tensile strength showed a decrease from 25 to 12 MPa with increasing LPA content. Though with excellent damping and mechanical properties, T_g of cured AE systems is above room temperature, at which the damping management is needed. This may limit its application and further research should be carried out. To sum up, the acrylate-based epoxy resin, with excellent combination properties, shows significant potential as novel and effective damping matrix to prepare intrinsic damping composites with excellent damping properties.

ACKNOWLEDGMENTS

The authors gratefully acknowledge supports of carefully revision of English from Dr. Lifang Zhang, measurements of DMTA from Zhiying Zhang, and the SEM characterization from Dr. Jincheng Pang. Author contributions: The manuscript was written through contributions of all authors. All authors have given approval of the final version of the manuscript. The authors declare no competing financial interest. These authors contributed equally to this work.

REFERENCES

1. Nikhil, K.; Bingqing, W.; Pulickel, M. A. *Adv. Mater.* **2002**, *14*, 13.
2. Wang, Y.; Zhan, M.; Li, Y.; Shi, M.; Huang, Z. *Polym. Plast. Tech. Eng.* **2012**, *51*, 840.
3. Haris, A. *J. Mater. Sci.* **2008**, *43*, 3289.
4. Wang, G.; Jiang, G.; Zhang, J. *Thermochim. Acta* **2014**, *589*, 197.
5. Tripathi, G.; Srivastava, D. *Mater. Sci. Eng. A* **2007**, *443*, 262.
6. Ji-Fang, F.; Li–Yi, S.; Shuai, Y.; Qing-Dong, Z.; Deng-Song, Z.; Yi, C.; Jun, W. *Polym. Adv. Technol.* **2008**, *19*, 1597.
7. Gu, J.; Wu, G.; Zhang, Q. *Mater. Sci. Eng. A* **2007**, *452*, 614.
8. Wang, T.; Chen, S.; Wang, Q.; Pei, X. *Mater. Des.* **2010**, *31*, 3810.
9. Hengshi, Z.; Xiaoxue, S.; Shiai, X. *J. Appl. Polym. Sci.* **2014**, *131*, 547.
10. Poornima, V. P.; Puglia, D.; Maria, H. J.; Kenny, J. M.; Thomas, S. *RSC Adv.* **2013**, *3*, 24634.
11. Bing, T.; Xiaobing, L.; Xiuli, Z.; Junhua, Z. *Appl. Polym. Sci.* **2014**, 40614.
12. Dai, J.-B.; Kuan, H.-C.; Du, X.-S.; Dai, S.-C.; Ma, J. *Polym. Int.* **2009**, *58*, 838.
13. Lu, S.; Li, S.; Yu, J.; Yuan, Z.; Qi, B. *RSC Adv.* **2013**, *3*, 8915.
14. Chen, Y.; Yao, D.; Zou, H.; Liang, M. *RSC Adv.* **2014**, *4*, 44750.
15. Alnefaie, K. A.; Aldousari, S. M.; Khashaba., U. A. *Compos. Part A* **2013**, *52*, 1.
16. Wang, T.; Chen, S.; Wang, Q.; Pei, X. *Design* **2010**, *31*, 3810.
17. Chen, S.; Wang, Q.; Wang, T.; Pei, X. *Mater. Des.* **2011**, *32*, 803.
18. Wenwen, Y.; Dezhi, Z.; Miao, D. *Eur. Polym. J.* **2013**, *49*, 1731.
19. Terenzi, A.; Vedova, C.; Lelli, G.; Mijovic, J.; Torre, L.; Valentini, L. *Compos. Sci. Technol.* **2008**, *68*, 1862.
20. Vahedi, V.; Pasbakhsh, P.; Siang-Piao, C. *Design* **2015**, *68*, 42.
21. Grant, I. D.; Lowe, A. T.; Thomas, S. *Compos. Struct.* **1997**, *38*, 581.
22. Wang, X.; Liu, H.; Yang, S. *Wuhan Univ. Technol. Mater. Sci. Ed.* **2008**, *23*, 411.
23. Hong, Z.; Xiang, W.; Zhao, X. *J. Wuhan Univ. Technol.* **2009**, *31*, 101.
24. Ratna, D.; Manoj, N. R.; Chandrasekhar, L.; Chakraborty, B. C. *Polym. Adv. Technol.* **2004**, *15*, 583.
25. Kim, D.; Centea, T.; Nutt, S. R. *Compos. Sci. Technol.* **2014**, *100*, 63.
26. Sudha, J. D.; Pradhan, S.; Viswanath, H.; Unnikrishnan, J.; Brahmbhatt, P.; Manju, M. S. *J. Therm. Anal. Calorim.* **2014**, *115*, 743.
27. Francis, B.; Lakshmana Rao, V.; Vanden Poel, G. *Polymer* **2006**, *47*, 5411.
28. Omrani, A.; Simon, L. C.; Rostami, A. A.; Ghaemy, M. *Eur. Polym. J.* **2008**, *44*, 769.
29. Lipatov, Y. S.; Tatiana, T. *Adv. Polym. Sci.* **2007**, *208*, 1.
30. Li, Q.; Huang, G.; Jiang, L. *Acta Polym. Sin.* **2003**, *3*, 409.
31. Xiao-xue, S.; Wen-jia, S.; Ji-chun, Y.; Li-ping, Z.; Xiao-jun, C.; Wen-yong, D.; Yong-jin, L. *Acta Polym. Sin.* **2012**, *11*, 1234.
32. Jim, G.; Simon, G. P.; Cook, W. D. *J. Appl. Polym. Sci.* **1999**, *72*, 1479.
33. Zhang, Y.; Adams, R. D.; da Silva, L., F. M. *J. Adhes.* **2014**, *90*, 327.
34. Xiaojun, H.; Jinrong, W.; Guangsu, H; Xiaoan, W. *J. Macro. Sci. B Phys.* **2011**, *50*, 188.
35. Zhang, R.; He, X.; Huang, G. *J. Polym. Res.* **2014**, *21*, 388.